

The Eddy Experiment II: GNSS-R speculometry for directional sea-roughness retrieval from low aircraft

O. Germain, G. Ruffini, F. Soulat, M. Caparrini,¹ B. Chapron² and P. Silvestrin³

We report on the retrieval of directional sea-roughness (the full directional mean square slope, including direction and isotropy) through inversion of Global Navigation Satellite System Reflections (GNSS-R) data collected during an experimental flight at 1 km altitude. The emphasis is on the utilization of the entire Delay-Doppler Map (DDM) in order to infer ocean roughness directional parameters. Obtained estimates are analyzed and compared to Jason-1 measurements and ECMWF numerical weather model outputs. We highlight the impact of long waves on scatterer velocity and the Delay Doppler spectrum.

1. Introduction

Several GNSS constellations and augmentation systems are presently operational or under development, including the pioneering US Global Positioning System (GPS) and the forthcoming European system, Galileo. These all-weather, long-term, stable and precise L-band signals can be used for bistatic remote sensing of the ocean surface, an emerging concept known as GNSS-R.

Among several applications, two classes have rapidly emerged in the community: sea-surface altimetry (see

Ruffini *et al.* [2004] and references therein) and sea-surface “speculometry” (a term discussed below), the determination of gravity wave sea roughness. Although this paper addresses the latter, we note here the intrinsic capability of GNSS-R for providing co-located measurements of both surface roughness and sea level with high spatial and temporal resolution. Co-location can help quantify the relationship of velocities in the upper ocean (as driven by wind stress forcing) with surface height dynamics.

As detected at L-band, the GNSS-R return is dominated by sea surface roughness elements at a scale for which gravitational attraction is the major restoring force. GNSS-R surface roughness measurements are therefore strongly correlated to the gravity dominated wave distribution.

In terms of operational applications, the expected relatively high spatial and temporal measurements can be used to constrain global ocean wave models (WAM) for better forecasts. With regards to scientific applications, sea roughness data can help quantify atmosphere-ocean coupling, including momentum and energy fluxes—e.g., through the drag coefficient for hurricane modeling—as well as surface wave acceleration, breaking/whitecapping and gas exchange. In particular, air-sea CO₂ flux is an important ingredient in understanding the ocean’s biogeochemical response to, and its influence on, climate change. As now understood and experimentally demonstrated, a very promising approach to quantify CO₂ flux will be to better quantify the surface fractional area, which is readily measurable from surface slope measurements. Recent studies at NASA/Wallops (FEDS.98, the Flux Exchange Dynamics Study) indicate that surface roughness (through its relation to Fractional Area) is a much better quantifier of the air sea gas flux than the traditionally used wind speed (Watson *et al.* [1999]). Using GNSS-R to extract gravity surface slope statistical properties, temporal spatial climatologies could be inferred to help quantify the role of the ocean in taking up increases of CO₂.

In addition, global L-band sea-roughness data is important for L-band radiometric missions, such as SMOS (Soil Moisture and Ocean Salinity) and AQUARIUS, in order to separate roughness and salinity contributions to L-band radiometric brightness measurements.

Inferring sea roughness from GNSS-R data requires (i) a parametric description of the sea surface, (ii) an electromagnetic and instrument model for sea-surface scattering at L-band and (iii) the choice of a GNSS-R data product to be inverted. In the literature, there is quite an agreement on the two first aspects. It has been recognized that the scattering of GNSS signals can be modeled as a Geometric Optics process (GO), where the fundamental physical process is the scattering from mirror-like surface elements. This is the reason for the use of the term “speculometry” here, which stems from the Latin word for mirror, *speculo*. Therefore, the most important features of the sea surface in GNSS-R are described by the statistics of facet slopes and their curvatures at scales larger than the electromagnetic wavelength (λ).

The statistical distribution of facet slopes is described by the bi-dimensional sea-surface slope probability density

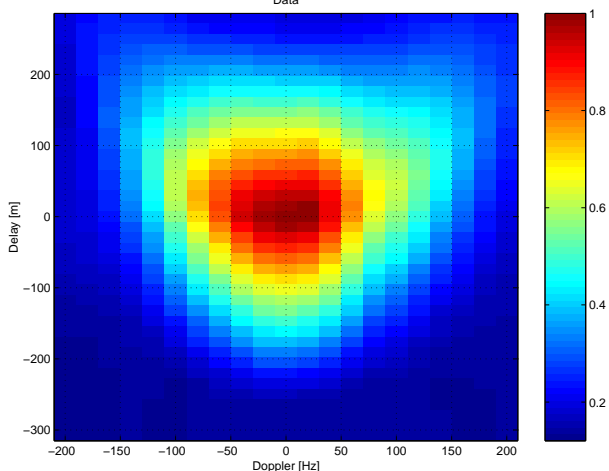


Figure 1. Example of GPS-R Delay-Doppler Map.

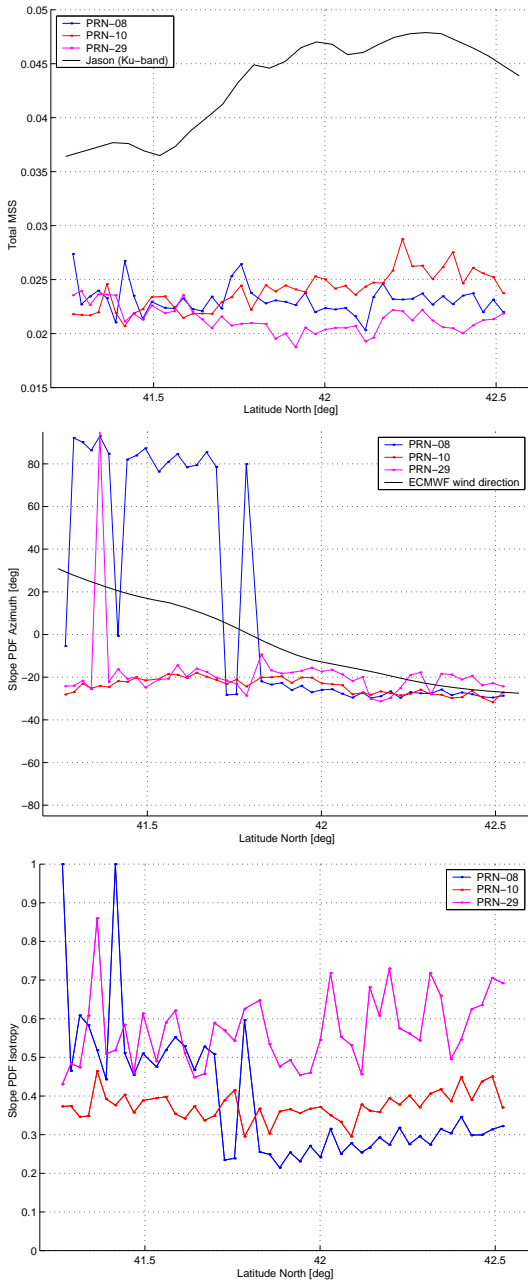


Figure 2. DMSS $_{\lambda}$ estimation with the DDM least-square inversion approach, along the descending (North to South) track—MSS top, SPA middle and SPI bottom. The total MSS (Ku-Band) measured by Jason-1 and the ECMWF wind direction are also shown for comparison.

function (PDF). Under a Gaussian assumption, three parameters suffice to fully define the PDF: the directional mean square slope DMSS $_{\lambda}$, which results from the integration of the ocean energy spectrum at wavelengths larger than λ . The symbol DMSS $_{\lambda}$ is a symmetric tensor which englobes the three parameters defining the ellipsoidal shape of the slope PDF: scale (total MSS), direction (Slope PDF azimuth) and isotropy (Slope PDF isotropy).

It is important to note that DMSS $_{\lambda}$ has rarely been emphasized as the geophysical parameter of interest in the literature. Instead, most authors link sea roughness to the near surface wind vector, which is thought to be more useful for

oceanographic and meteorological users. Unfortunately, this is somewhat misleading, as the relationship between surface wind and roughness is not one-to-one and requires an additional modeling layer. The connection between DMSS $_{\lambda}$ and wind is affected by other factors (e.g., swell, fetch and degree of maturity), as is well known in the altimeter community (see *Gourrion et al.* [2002]).

Also, for simplicity the product typically inverted in GNSS-R speculometry is a simple Delay Waveform, that is, a 1D delay map of the reflected signal amplitude. Using a single GNSS emitter, the wind speed can be inferred assuming an isotropic slope PDF (see, e.g., *Komjathy et al.* [2000], *Garrison et al.* [1998, 2002], or *Cardellach et al.* [2003]). Attempts have also been made to measure the wind direction by fixing the PDF isotropy to some theoretical value (around 0.7) and using at least two satellites reflections with different azimuths (see, e.g., *Zuffada et al.* [2000], *Armatys et al.* [2000] and *Garrison et al.* [2003]).

As investigated in the frame of the ESA OPPSCAT project (*Ruffini et al.* [2000]), it is possible to work with a product of higher information content, the 2D DDM of the reflected signal amplitude. The provision of an extra dimension opens the possibility of performing a robust estimation of all the DMSS $_{\lambda}$ parameters. In *Elfouhaily et al.* [2002], a simple and rapid method based on the moments of the DDM was proposed to estimate the full set of DMSS $_{\lambda}$. Unfortunately, this approach neglects the impact of the bistatic Woodward Ambiguity Function and antenna gain modulation and provides only a first order approximation solution.

Here we focus on a direct fitting/inversion of the DDM for the retrieval of directional roughness, and analyze GNSS-R data collected during the Eddy Experiment. The campaign and altimetric data analysis of this experiment is reported in *Ruffini et al.* [2004] and *Soulat* [2003] (where the analysis of optical data was also carried out). The primary goal of the paper is to investigate the full exploitation of the bidimensional GNSS-R DDM product to infer the set of three DMSS $_{\lambda}$ parameters. The driver of the study has been the exhaustive exploitation of the information contained in the DDM product. The approach here relies on a least-squares fit of the speculometric model, as discussed in the third section. In the fourth section, results are compared to ancillary data (Jason-1 radar altimeter, ECMWF numerical weather model). Finally, another important outcome of the paper is put forward: we show good evidence that a small part of the DDM Doppler spread can be attributed to the “scatterer velocity”, i.e., the rapid motion of the λ (or larger) sized sea-surface facets following the long waves.

2. Data collection and pre-processing

As discussed in *Ruffini et al.* [2004], the data set (i.e. direct and reflected GPS signals together with the aircraft kinematic data) was gathered during an airborne campaign carried out in September 2002. The aircraft overflew the Mediterranean Sea, off the coast of Catalonia (Spain), northwards from the city of Barcelona for about 150 km at 1000 m altitude and 45–75 m/s speed. The area is crossed by the ground track #187 of the Jason-1 radar altimeter, which the aircraft overflew during the satellite overpass, for precise comparison. The track was overflown twice, first during the ascending pass (from South to North) at low speed (45–60 m/s) and second during the descending pass (from North to South) at a faster speed (65–75 m/s) due to wind. The time shift between the two passes over a same point on the track ranged from 45 min to 2 h 15 min. During the ascending pass, PRNs 08, 10 and 24 were visible with elevations spanning 30° to 85° while PRNs 08, 10 and 29 were visible

during the descending track with elevations between 40° and 75° . The configuration of this test flight was not optimized for speculometry: from such low altitude, the sea-surface reflective area is essentially limited by the PRN C/A code, and the glistening zone is coarsely Delay-Doppler mapped.

The raw GPS signals were acquired with a modified TurboRogue receiver, sampled at 20.456 MHz and pre-processed with a dedicated software composed of two sub-units fed with the direct and reflected signals. Correlations were computed along 81 delay lags while the Doppler dimension spanned -200 to 200 Hz with a step of 20 Hz. The coherent/incoherent integration times were respectively set to 20 milliseconds and 10 s, meaning that the averaged DDM were produced at the rate of 0.1 Hz after summation of 500 incoherent looks (see Figure 1 for a sample waveform).

3. Speculometric model and DDM inversion

In the *Zavorotny et al.* [2000] GNSS-R GO model, the link between the DDM mean power at delay-Doppler $P(\tau, f)$ and the sea-surface slope PDF $\mathcal{P}(s_x, s_y)$ is given by

$$P(\tau, f) = \int dx dy \frac{G_r}{R_t^2 R_r^2} \cdot \frac{q^4}{q_z^4} \cdot \mathcal{P} \left(\frac{-q_x}{q_z}, \frac{-q_y}{q_z} \right) \cdot \chi^2 [\tau_m(x, y) - \tau_c - \tau, f_m(x, y) - f_c - f], \quad (1)$$

where G_r is the receiver antenna pattern, R_t and R_r the distances from generic point on sea-surface to transmitter and receiver, (q_x, q_y, q_z) the scattering vector, χ the Woodward Ambiguity Function (WAF), \mathcal{P} the slope PDF, $\tau_m(x, y)$ and $f_m(x, y)$ the delay-Doppler mapping on sea-surface and (τ_c, f_c) the extra delay/Doppler of the geometric specular-point with respect to direct signal (also called DDM “centers”). Accounting for the receiver mean thermal noise P_N and including a scaling parameter α , the mean amplitude of the DDM can be written as $A(\tau, f) = \sqrt{\alpha P(\tau, f) + P_N}$. As discussed above, \mathcal{P} is described by the DMSS_λ parameter set, which defines an elliptic quadratic form in the 2D space of slopes. Mean-square slopes along major and minor principal axes are often called MSS up-wind (mss_u) and MSS cross-wind (mss_c) respectively. In the following, we will refer to the Total MSS ($\text{MSS}_{tot} = 2\sqrt{mss_u \cdot mss_c}$, proportional to the ellipse area), the Slope PDF azimuth (SPA, the direction of semi-major axis with respect to North) and the Slope PDF Isotropy (SPI, equal to mss_c/mss_u).

The data inversion was performed through a minimization of the mean square difference between model and data DDMs. Numerical optimization was carried out by a steepest-slope-descent algorithm with a Levenberg-Marquardt type adjustment. The main difficulty stemmed from the presence of several nuisance parameters in the forward model (mainly τ_c and f_c but also α). The DDM centers were affected by the aircraft trajectory (altitude and vertical velocity) to first order but also by geophysical parameters (sea level, currents, etc.). They needed to be accurately known in order to estimate DMSS_λ . For this reason, the DMSS_λ and nuisance parameters were jointly estimated in an iterative manner.

4. Results and analysis

The values of DMSS_λ estimated along the descending track of the flight are shown on Figure 2. The top plot illustrates the variations of total MSS. As observed, the inter-PRN consistency is reasonable in the southern part of the track but worsens slightly in the northern part. For comparison, the total MSS in Ku-band was derived from

the Jason-1 σ^0 co-located measurements at 1 Hz sampling (7 km) and 20 km resolution. The Jason-1 MSS was obtained through the simple relationship $\text{MSS} = \kappa/\sigma^0$, κ being the effective (empirical) Fresnel coefficient, here set to 0.45. As expected, we observed that the level and dynamic of MSS decreased with longer wavelength (from 2 cm in Ku-band to 19 cm in L-band). The low dynamic of L-band MSS impeded any clear trend comparison although the measurements of PRN-10 seem in good agreement with Jason-1. The Jason-1 wind speed, derived from both the Ku-band σ^0 and the significant wave height (of about 2 m), ranged from 9 to 13 m/s along the track. Translating this wind speed into L-band MSS through the spectrum of *Elfouhaily et al.* [1997] yields values between 0.0220 and 0.0255, in-line with GNSS-R results. However, we emphasize that the assumption of a wind-driven spectrum was not really warranted during the campaign: the presence of swell definitely had a significant impact.

SPA estimation results are presented on the middle plot. The inter-PRN consistency is here very satisfying and the apparent discrepancy in the southern part of the track can be explained as a degenerate solution of the estimation problem. The inversion of DDM for the SPA is degenerate in at least two cases: when the transmitter is at zenith or when the receiver moves towards the transmitter. In these scenarios, the Delay-Doppler lines mapping the glistening zone are fully symmetric around the receiver direction and it becomes impossible to distinguish a slope PDF from its mirror image about the receiver direction. This effect is clearly observed here where the two found SPA (-20° and 80°) are indeed symmetric around the aircraft heading direction (30°). In this part of the track, the azimuth of PRN-08 is about 50° , almost aligned with the aircraft heading direction. In the northern part of the track, the estimated SPA matches very well with the wind direction provided by ECMWF. In the southern part, the mismatch reaches up to 50° . However, we underline that wind is not the only element driving SPA and that swell also contributed in this case. Besides, the accuracy of ECMWF wind direction is estimated to 20° .

Finally, the bottom plot shows the SPI variations along the track. It is worth pointing out that the wind-driven spectrum of *Elfouhaily et al.* [1997] for a mature sea predicts a SPI value around 0.65, largely insensitive to wind

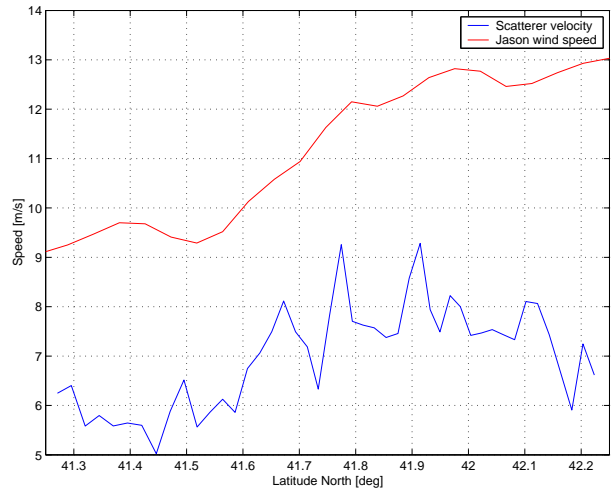


Figure 3. Average scatterer velocity obtained when assuming a perfect match of ascending/descending MSS and the first order MSS model. It correlates fairly well with wind speed and the observed swell from optical data.

speed. The significant departure from this reference value is a probable signature of under-developed sea with the presence of swell. However, the poor consistency among PRN remains an issue. Further work is needed to validate the accuracy of SPI estimation and to better understand the potential information contained in this product.

As a second outcome of this campaign analysis, we now discuss the signature of “scatterer velocity” in the data, i.e., the signature of fastly moving sea-surface facets with size (curvature) larger than ~ 20 cm. Such signature was discovered when comparing the total MSS along the ascending and descending tracks, as estimated by the least-squares approach: a drastic discrepancy (up to 33%) was observed for two passes shifted by less than hour over the same track point. As a simple check, we inverted the data with the simpler first-order analytic method proposed in *Elfouhaily et al.* [2002], $MSS = \lambda^2 B^2 / (2V^2 \sin^2 \epsilon)$, where ϵ is the transmitter elevation, V is the receiver speed and B is the DDM Doppler bandwidth: the results do resemble the ones obtained with the least-squares approach and the ascending/descending discrepancy remains.

Multipath effects could conceivably lead to a Doppler width modulation. However, some azimuth dependence should have been observed and was not. Another possible cause could be a changing aircraft attitude between ascending and descending tracks, but the aircraft roll and pitch values were checked to be nominal along both tracks. Moreover, a change in yaw would slightly impact the antenna pattern ground projection but would translate only into a Doppler bandwidth cut and never a broadening. The most likely explanation was that of a geophysical signature: the Doppler spectrum width was modulated by the motion of specular facets on sea-surface. While the inversion approach assumed a still surface, the relative velocity between receiver and scatterer should be taken into account for proper DDM inversion. At high receiver velocities this assumption is fine because the scatterer velocity impact will not be significant. At the low speeds in the Eddy Experiment, however, scatterer velocity becomes relevant. This analysis is consistent with the fact that the MSS estimated in the ascending track (slower aircraft speed, from 45 to 60 m/s) showed abnormal high values compared to the ones estimated during the ascending track (faster speed, from 65 to 75 m/s).

Assuming that the MSS did not vary significantly between the times of the ascending and descending passes, we can roughly solve for the scatterer velocity v_s (assumed here to point along the track for simplicity) using the first order equation $MSS = \lambda^2 B^2 / (2V^2 \sin^2 \epsilon)$ and considering the relative velocity between sea-surface scatterers and aircraft, i.e., $V \pm v_s$ for the ascending/descending passes. Using this scheme with all possible pairs of measurements and averaging, the plot of Figure 3 results. The scatterer velocity variations correlate well with the variations of wind speed. From the dispersion relation, the average speed of 8 m/s corresponds to long waves of about 45 m wavelength, a result consistent with optical observations of the swell vector (wavelength and direction, see *Soulat* [2003]). A more detailed analysis can be carried out taking into account the correct deformation of the Doppler lines on the surface and searching for a scatterer velocity vector.

5. Conclusion

We have reported the first inversion of GNSS-R full Delay-Doppler Maps for the retrieval of the sea-surface directional mean square slope, $DMSS_\lambda$. The estimates have shown good inter-PRN consistency (except for SPI) and fair agreement with other sources of data.

In addition, we have discussed a new geophysical signature in GNSS-R: the sea-surface scatterer velocity. Sea-surface scatterers can easily travel at velocities reaching 5-10

m/s and their motion may impact the DDM Doppler bandwidth of slow-moving receivers. The detection of such a geophysical signature opens new opportunities for GNSS-R speculometry: to measure either $DMSS_\lambda$ or a combination of $DMSS_\lambda$ and scatterer velocity, depending on the aircraft speed.

Finally, we emphasize that the flight was not optimized for speculometry: higher and faster flights are needed in the future in order to consolidate the concept of DDM inversion for $DMSS_\lambda$ estimation and to test new concepts for increased inversion resolution.

Acknowledgments. The data analysis and the experimental campaign were respectively carried out under the ESA contracts TRP-ETP-137.A and 3-10120/01/NL/SF (OPPSCAT). We thank the Institut Cartografic de Catalunya for flawless flight operations and aircraft GPS/INS kinematic processing. All Starlab authors have contributed significantly; the Starlab author list has been ordered randomly.

References

Armatys, M., A. Komjathy, P. Axelrad, and S. Katzberg. A comparison of GPS and scatterometer sensing of ocean wind speed and direction. In *Proc. IEEE IGARSS*, Honolulu, HA, 2000.

Cardellach, E., G. Ruffini, D. Pino, A. Rius, A. Komjathy, and J. Garrison, Mediterranean balloon experiment: GPS reflection for wind speed retrieval from the stratosphere. *Rem. Sens. Env.*, 2003.

Elfouhaily, T., B. Chapron, K. Katsaros, and D. Vandemark, A unified directional spectrum for long and short wind-driven waves, *JGR*, 102(15):781–796, 1997.

Elfouhaily, T., D. Thompson, and L. Linstrom, Delay-Doppler analysis of bistatically reflected signals from the ocean surface: Theory and application. *IEEE TGRS*, 40(3):560–573, 2002.

Garrison, J.L., Katzberg, J.L., Effects of sea roughness on bistatically scattered range coded signals from the Global Positioning System, *GRL*, vol 25, n. 13, 1998.

Garrison, J.L., Wind speed measurement using forward scattered GPS signals. *IEEE TGRS*, 40:50–65, 2002.

Garrison, J.L., Anisotropy in Reflected GPS Measurements of Ocean Winds, in *Proceedings of the 2003 Workshop on Oceanography with GNSS-R*, Starlab, July 2003. Available at <http://starlab.es/gnssr2003/proceedings/>.

Gourrion, J., D. Vandemark, S. Bailey, and B. Chapron, Investigation of C-band altimeter cross section dependence on wind speed and sea state, *Can. J. Remote Sensing*, Vol. 28, No. 3, pp. 484–489, 2002.

Komjathy, A., V. Zavorotny, P. Axelrad, G.H. Born, and J.L. Garrison, GPS signal scattering from sea surface: Wind speed retrieval using experimental data and theoretical model. *Rem. Sens. Env.*, 73:162–174, 2000.

Ruffini, G., J.L. Garrison, E. Cardellach, A. Rius, M. Armatys, and D. Masters, Inversion of GPS-R delay-Doppler mapping waveforms for wind retrieval. In *Proc. IEEE IGARSS*, Honolulu, HA, 2000.

Ruffini, G., F. Soulat, M. Caparrini, O. Germain and M. Martin-Neira, The Eddy Experiment I: Accurate GNSS-R ocean altimetry from low altitude aircraft, to appear in *GRL*, 2004.

Soulat, F., Sea surface remote-sensing with GNSS and sunlight reflections, *Doctoral Thesis*, Universitat Politècnica de Catalunya/Starlab, 2003. Available at <http://starlab.es/library.html>.

Watson W. G., et al., NASA/GODDARD Research Activities for the Global Ocean Carbon Cycle: A Prospectus for the 21st Century, December 99.

Zavorotny V., and A. Voronovich, Scattering of GPS signals from the ocean with wind remote sensing application, *IEEE TGRS*, 38(2):951–964, 2000.

Zuffada, C., and T. Elfouhaily, Determining wind speed and direction with ocean reflected GPS signals, In *Proc. of Sixth Int. Conf. on Remote Sensing for Marine and Coastal Environments*, Charleston, 2000.